Northumbria Research Link

Citation: Fu, Yichuan, Gao, Zhiwei, Wu, Haimeng, Yin, Xiuxia and Zhang, Aihua (2021) Data-Driven Fault Classification for Non-Inverting Buck–Boost DC–DC Power Converters Based on Expectation Maximisation Principal Component Analysis and Support Vector Machine Approaches. In: 1st IEEE International Power Electronics and Application Symposium, IEEE PEAS'2, 12-15 Nov 2021, Shanghai, China. (In Press)

URL:

This version was downloaded from Northumbria Research Link: http://nrl.northumbria.ac.uk/id/eprint/47253/

Data-Driven Fault Classification for Non-Inverting Buck–Boost DC–DC Power Converters Based on Expectation Maximisation Principal Component Analysis and Support Vector Machine Approaches

Yichuan Fu[*†], Zhiwei Gao[*†], Haimeng Wu[*†], Xiuxia Yin[‡], and Aihua Zhang[§]

[*]*Faculty of Engineering and Environment, Department of Mathematics, Physics and Electrical Engineering*
University of Northumbria at Newcastle, Newcastle upon Tyne, Tyne and Wear, NE1 8ST, United Kingdom
[†]E-mail: {y.fu, zhiwei.gao, and haimeng.wu}@northumbria.ac.uk
[‡]*Department of Mathematics*, *School of Science*, *Nanchang University*
Nanchang, Jiangxi Province, 330031, P. R. China, E-mail: yinxiuxia@ncu.edu.cn
[§]*College of Engineering*, *School of Physical Science and Technology*, *Bohai University*
Jinzhou, Liaoning Province, 121000, P. R. China, E-mail: jsxinxi_zah@163.com

Abstract—**Data-driven fault classification for power converter systems has been taking more into considerations in power electronics, machine drives, and electric vehicles. It is challenging to classify the different topologies of faults in the real-time monitoring control systems. In this paper, a data-driven and supervised machine learning-based fault classification technique is adopted by combining and consolidating with Expectation Maximisation Principal Component Analysis (EMPCA) and Support Vector Machine (SVM) to substantiate the availability of fault classification. The proposed methodology is applied to the non-inverting Buck–Boost DC–DC power converter systems subjected to the incipient fault and serious fault, respectively. Finally, the feasibility of the approach is validated by intensive simulations and comparison studies.**

Keywords—**Data-driven, fault classification, expectation maximisation principal component analysis, support vector machine, non-inverting Buck–Boost DC–DC power converters.**

I. Introduction

During the two decades, real-time monitoring, fault diagnosis, prognosis, and resilient control perform critical roles in power electronics, machine drives, electric vehicles, and networked control systems, ensuring availability, enhancing reliability, and reducing maintenance costs [1]–[4]. Fault diagnosis methods can be categorised into four aspects: model-based algorithm, signal-based approach, knowledge-based technique, and hybrid applications [1], [3]. All the methodologies mentioned above need the information recorded in the input and output signals. However, the knowledge-based algorithm relies more on data processing and data-based learning, including historical processing data and real-time data. Therefore, the knowledge-based fault diagnosis technique is also determined by the data-driven method [1], [3].

Condition monitoring, fault detection, and fault diagnosis methods are widely applied in DC–DC power converter systems [5]–[13]. In this paper, we concentrated on

both incipient and serious fault classifications for the non-inverting Buck–Boost DC–DC power converter systems subjected to capacitor faulty conditions in terms of combining and consolidating with Expectation Maximisation Principal Component Analysis (EMPCA) and Support Vector Machine (SVM) strategies. The experimental datasets/samples, including healthy and faulty scenarios, are generated by the non-inverting Buck–Boost DC–DC power converter systems with Additive White Gaussian Noise (AWGN) signals. Numerous simulation studies are carried out with detailed result analyses and discussions.

The rest of this paper is organised as follows: Section II introduces the basic concepts and fundamentals of the non-inverting Buck–Boost DC–DC power converter systems. Section III demonstrates the proposed methodologies, which are PCA Plus SVM (PCA + SVM) and EMPCA Plus SVM (EMPCA + SVM). Experimentation designs and simulation results are respectively presented in Section IV and Section V. Finally, this paper ends by summarising the conclusion in Section VI.

II. Non-Inverting Buck–Boost DC–DC Power Converter Systems

We considered the non-inverting Buck–Boost DC–DC power converter systems, which is depicted in Fig. 1. Incipient and serious fault classification performances for the non-inverting Buck–Boost DC–DC power converters were estimated in Section V, subjected to faulty capacitance conditions according to the different topologies of data-driven and supervised machine learning-based methods, which are PCA + SVM and EMPCA + SVM, respectively.

Experimental samples/datasets, which contain healthy and faulty conditions, are generated by the aforementioned non-inverting Buck–Boost DC–DC power converter systems.
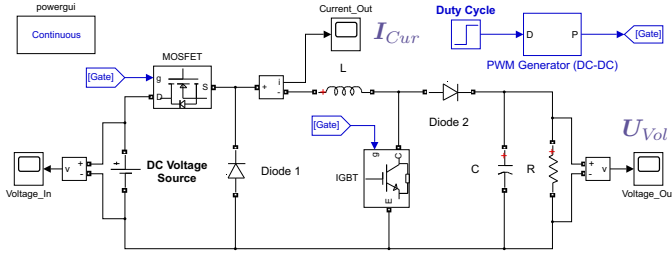
Fig. 1. The MATLAB/SIMULINK block diagram of the non-inverting Buck–Boost DC–DC power converter systems.

III. METHODOLOGIES

A. Conventional Principal Component Analysis

The non-inverting Buck–Boost DC–DC power converter is used to generate a dataset; either the output current signals (I_{Cur}) or output voltage signals (U_{Vol}) are employed to establish a first-order vector [14], [15]:

$$I_{Cur} = [I_{Cur\_1}, I_{Cur\_2}, \ldots, I_{Cur\_n}]^T \in \mathcal{R}^{n \times 1} \quad (1)$$

$$U_{Vol} = [U_{Vol\_1}, U_{Vol\_2}, \ldots, U_{Vol\_n}]^T \in \mathcal{R}^{n \times 1} \quad (2)$$

where n is the number of features. Therefore, the vector model can be represented as $X_{Cur} = [I_{Cur\_1}, I_{Cur\_2}, \ldots, I_{Cur\_n}]^T$ (3) or $X_{Vol} = [U_{Vol\_1}, U_{Vol\_2}, \ldots, U_{Vol\_n}]^T$ (4) [14], [15].

The objectives of PCA technique are shown in the following below [14], [15]:

❖ Linear projection to a lower-dimensional subspace;
❖ Maximise the variance of the projected data;
❖ Minimise the discrepancy of the full-dimensional data and the projection in the subspace.

Due to the restriction of the page, the basic concepts and fundamentals of the PCA algorithm are omitted. References [14] and [15] demonstrate the derivations and computation processes of the conventional PCA technique.

B. Expectation Maximisation Principal Component Analysis

Procedure 1: Gaussian Mixture.

Denote $\mathbf{x} = (\mathbf{x}_1, \mathbf{x}_2, \ldots, \mathbf{x}_n)$ as a sample of n independent observations from a mixture of two multivariate normal distributions of dimension d, and simultaneously, define $\mathbf{z} = (z_1, z_2, \ldots, z_n)$ as the latent variables that determine the component from which the observation originates as follows [16]–[19]:

$$X_i \mid (Z_i = 1) \sim \mathcal{N}_d(\boldsymbol{\mu}_1, \boldsymbol{\Sigma}_1) \quad (5)$$

$$X_i \mid (Z_i = 2) \sim \mathcal{N}_d(\boldsymbol{\mu}_2, \boldsymbol{\Sigma}_2) \quad (6)$$

$$X_i \mid (Z_i = n) \sim \mathcal{N}_d(\boldsymbol{\mu}_n, \boldsymbol{\Sigma}_n) \quad (7)$$

where $\mathbb{P}(Z_i = 1) = \tau_1$ (8), $\mathbb{P}(Z_i = 2) = \tau_2 = 1 - \tau_1$ (9), $\mathbb{P}(Z_i = n) = \tau_n = 1 - \tau_{n-1}$ (10) [16]–[19].

The aim is to estimate the unknown parameters representing the *mixing value* between the Gaussians and the means and covariances of each θ [16]–[19]:

$$\theta = (\boldsymbol{\tau}, \boldsymbol{\mu}_1, \boldsymbol{\mu}_2, \ldots, \boldsymbol{\mu}_n, \boldsymbol{\Sigma}_1, \boldsymbol{\Sigma}_2, \ldots, \boldsymbol{\Sigma}_n) \quad (11)$$

where the *incomplete-data* likelihood function can be calculated as follows [16]–[19]:

$$L(\theta; \mathbf{x}) = \prod_{i=1}^{n} \sum_{j=1}^{2} \tau_j \, f(\mathbf{x}_i; \boldsymbol{\mu}_j, \boldsymbol{\Sigma}_j) \quad (12)$$

and the *complete-data* likelihood function can be represented in the following below [16]–[19],

$$L(\theta; \mathbf{x}, \mathbf{z}) = \prod_{i=1}^{n} \prod_{j=1}^{2} [f(\mathbf{x}_i; \boldsymbol{\mu}_j, \boldsymbol{\Sigma}_j)\tau_j]^{\mathbb{I}(z_i=j)} \quad (13)$$

or alternatively [16]–[19],

$$L(\theta; \mathbf{x}, \mathbf{z}) = \exp \left\{ \sum_{i=1}^{n} \sum_{j=1}^{2} \mathbb{I}(z_i = j) \left[\log \tau_j - \tfrac{1}{2} \log |\boldsymbol{\Sigma}_j| - \right. \right.$$
$$\left. \left. \tfrac{1}{2}(\mathbf{x}_i - \boldsymbol{\mu}_j)^T \boldsymbol{\Sigma}_j^{-1}(\mathbf{x}_i - \boldsymbol{\mu}_j) - \tfrac{d}{2} \log(2\pi) \right] \right\} \quad (14)$$

where $\mathbb{I}$ is an indicator function, and f is the probability density function of a multivariate normal. In the last equality, for each i, one indicator $\mathbb{I}(z_i = j)$ is equal to zero, and one indicator is equal to one. The inner sum thus reduces to one term [16]–[19].

Procedure 2: Expectation Step (E-Step).

Given a current estimation of the parameters $\theta^{(t)}$, the conditional distribution of the Z_i is determined by Bayes theorem to be the proportional height of the normal density weighted by τ [16]–[19]:

$$T_{j,i}^{(t)} := \mathbb{P}(Z_i = j \mid X_i = \mathbf{x}_i; \theta^{(t)})$$
$$= \frac{\tau_j^{(t)} \, f\left(\mathbf{x}_i; \boldsymbol{\mu}_j^{(t)}, \boldsymbol{\Sigma}_j^{(t)}\right)}{\tau_1^{(t)} \, f\left(\mathbf{x}_i; \boldsymbol{\mu}_1^{(t)}, \boldsymbol{\Sigma}_1^{(t)}\right) + \tau_2^{(t)} \, f\left(\mathbf{x}_i; \boldsymbol{\mu}_2^{(t)}, \boldsymbol{\Sigma}_2^{(t)}\right)} \quad (15)$$

These are so-called the '*membership probabilities*', which are typically considered the output of the **E-Step** (although this is not the Q function of below). This **E-Step** corresponds with setting up this function for Q [16]–[19]:

$$Q(\theta \mid \theta^{(t)}) = \mathbb{E}_{\mathbf{Z}|\mathbf{X}, \theta^{(t)}}[\log L(\theta; \mathbf{x}, \mathbf{Z})]$$
$$= \mathbb{E}_{\mathbf{Z}|\mathbf{X}, \theta^{(t)}} \left[\sum_{i=1}^{n} \log L(\theta; \mathbf{x}_i, Z_i) \right]$$
$$= \sum_{i=1}^{n} \mathbb{E}_{Z_i|\mathbf{X}; \theta^{(t)}}[\log L(\theta; \mathbf{x}_i, Z_i)]$$
$$= \sum_{i=1}^{n} \sum_{j=1}^{2} P(Z_i = j \mid X_i = \mathbf{x}_i; \theta^{(t)}) \log L(\theta_j; \mathbf{x}_i, j)$$
$$= \sum_{i=1}^{n} \sum_{j=1}^{2} T_{j,i}^{(t)} \left[\log \tau_j - \tfrac{1}{2} \log |\boldsymbol{\Sigma}_j| - \tfrac{1}{2}(\mathbf{x}_i - \boldsymbol{\mu}_j)^T \cdot \right.$$
$$\left. \boldsymbol{\Sigma}_j^{-1}(\mathbf{x}_i - \boldsymbol{\mu}_j) - \tfrac{d}{2} \log(2\pi) \right] \quad (16)$$

The expectation of $\log L(\theta; \mathbf{x}_i, Z_i)$ inside the sum is taken concerning the probability density function $\mathbb{P}(Z_i \mid X_i = \mathbf{x}_i; \theta^{(t)})$, which might be different for each $\mathbf{x}_i$ of the training sets. Everything in the **E-Step** is known before the step is taken except $T_{j,i}$ computed according to the equation at the beginning of the **E-Step** section. Due to the fact that τ and $\boldsymbol{\mu}/\boldsymbol{\Sigma}$ appears in separate linear terms and can thus be maximised independently, the full conditional expectation does not need to be calculated in one step [16]–[19].

Procedure 3: Maximisation Step (M-Step).

$Q(\theta \mid \theta^{(t)})$ being quadratic in form means that determining the maximising values of θ is relatively straightforward. Alternatively, τ, $(\boldsymbol{\mu}_1, \boldsymbol{\Sigma}_1)$, and $(\boldsymbol{\mu}_2, \boldsymbol{\Sigma}_2)$ may all be maximised independently since they all appear in separate linear terms, which has the constraint of $\tau_1 + \tau_2 = 1$ [16]–[19]:

$$\boldsymbol{\tau}^{(t+1)} = \arg\min_{\boldsymbol{\tau}} Q(\theta \mid \theta^{(t)})$$
$$= \arg\min_{\boldsymbol{\tau}} \left\{ \left[\sum_{i=1}^{n} T_{1,i}^{(t)} \right] \log \tau_1 + \left[\sum_{i=1}^{n} T_{2,i}^{(t)} \right] \log \tau_2 \right\} \quad (17)$$

It has the same structure as the maximum likelihood estimation (MLE) for the binomial distribution. Therefore, we have [16]–[19]:

$$\tau_j^{(t+1)} = \frac{\sum_{i=1}^{n} T_{j,i}^{(t)}}{\sum_{i=1}^{n} \left(T_{1,i}^{(t)} + T_{2,i}^{(t)} \right)} = \frac{1}{n} \sum_{i=1}^{n} T_{j,i}^{(t)} \quad (18)$$

For the subsequent estimations of $(\boldsymbol{\mu}_1, \boldsymbol{\Sigma}_1)$ [16]–[19]:

$$\left(\boldsymbol{\mu}_1^{(t+1)}, \boldsymbol{\Sigma}_1^{(t+1)} \right) = \arg\min_{\boldsymbol{\mu}_1^{(t)}, \boldsymbol{\Sigma}_1^{(t)}} Q(\theta \mid \theta^{(t)})$$
$$= \arg\min_{\boldsymbol{\mu}_1^{(t)}, \boldsymbol{\Sigma}_1^{(t)}} \sum_{i=1}^{n} T_{1,i}^{(t)} \left\{ -\tfrac{1}{2} \log |\boldsymbol{\Sigma}_j| - \tfrac{1}{2} (\mathbf{x}_i - \boldsymbol{\mu}_j)^T \cdot \right.$$
$$\left. \boldsymbol{\Sigma}_j^{-1} (\mathbf{x}_i - \boldsymbol{\mu}_j) - \tfrac{d}{2} \log(2\pi) \right\} \quad (19)$$

It has the same architecture as a weighted MLE for a normal distribution. As a consequence, we have: $\boldsymbol{\mu}_1^{(t+1)} = (\sum_{i=1}^{n} T_{1,i}^{(t)} \mathbf{x}_i)/(\sum_{i=1}^{n} T_{1,i}^{(t)})$ (20) [16]–[19], and

$$\boldsymbol{\Sigma}_1^{(t+1)} = \frac{\sum_{i=1}^{n} T_{1,i}^{(t)} \left(\mathbf{x}_i - \boldsymbol{\mu}_1^{(t+1)} \right) \cdot \left(\mathbf{x}_i - \boldsymbol{\mu}_1^{(t+1)} \right)^T}{\sum_{i=1}^{n} T_{1,i}^{(t)}} \quad (21)$$

hence, by equilibrium $\boldsymbol{\mu}_2^{(t+1)} = (\sum_{i=1}^{n} T_{2,i}^{(t)} \mathbf{x}_i)/(\sum_{i=1}^{n} T_{2,i}^{(t)})$ (22) [16]–[19], $\boldsymbol{\Sigma}_2^{(t+1)}$ can be calculated as follows [16]–[19]:

$$\boldsymbol{\Sigma}_2^{(t+1)} = \frac{\sum_{i=1}^{n} T_{2,i}^{(t)} \left(\mathbf{x}_i - \boldsymbol{\mu}_2^{(t+1)} \right) \cdot \left(\mathbf{x}_i - \boldsymbol{\mu}_2^{(t+1)} \right)^T}{\sum_{i=1}^{n} T_{2,i}^{(t)}} \quad (23)$$

Procedure 4: Termination.

For termination, the iterative process should be satisfied by the following inequality [16]–[19]:

$$\mathbb{E}_{Z|\theta^{(t)}, \mathbf{x}} [\log L(\theta^{(t)}; \mathbf{x}, \mathbf{Z})]$$
$$\leq \mathbb{E}_{Z|\theta^{(t-1)}, \mathbf{x}} [\log L(\theta^{(t-1)}; \mathbf{x}, \mathbf{Z})] + \varepsilon \quad (24)$$

where ε indicates the assumed threshold [16]–[19].

C. Support Vector Machine

SVM algorithm was first introduced by Corinna Cortes and Vladimir N. Vapnik in 1995 [20], whose functionality was to demonstrate a variety of distinctive superiorities of solving problems, including small-sample, non-linear, and high-dimensional pattern recognition, respectively [20]–[23].

Consider an n-class problem. For a one-against-all (*One vs. All*) SVM, we determine n direct decision functions that separate one class from the remaining classes. Suppose the k-th decision function with the maximum margin, and the hyperplane decision function $H_k(\mathbf{x})$ can be mathematically represented in the following below [20]–[23],

$$H_k(\mathbf{x}) = \mathbf{w}_k^T \boldsymbol{\varphi}(\mathbf{x}) + b_k \quad (25)$$

where $\mathbf{w}_k$ is the p-dimensional vector, $\boldsymbol{\varphi}(\mathbf{x})$ is the mapping function which projects $\mathbf{x}$ into the p-dimensional feature subspace, and b_k is the bias component [20]–[23]. Therefore, $\mathbf{w}_k$ and b_k are the solutions to the problem [20]–[23]:

$$\min_{\mathbf{w}_k, b_k} \frac{1}{2} \|\mathbf{w}_k\|^2 + C \sum_{k=1}^{p_1 + p_2}$$

$$\textbf{s.t.} \quad y_k H_k(\mathbf{x}) \geq 1 - \varsigma_k, \qquad k = 1, 2, \ldots, p_1 + p_2$$
$$\varsigma_k \geq 0, \qquad\qquad k = 1, 2, \ldots, p_1 + p_2 \quad (26)$$

The hyperplane $H_k(\mathbf{x}) = 0$ forms the optimal separating hyperplane, and if the classification problem is separable, the training data belonging to class k satisfy $H_k(\mathbf{x}) \geq 1$ and those belonging to the remaining classes satisfy $H_k(\mathbf{x}) \leq -1$. Significantly, support vectors satisfy $|H_k(\mathbf{x})| = 1$. If the problem is inseparable, *unbounded* support vectors satisfy $|H_k(\mathbf{x})| = 1$ and *bounded* support vectors belonging to class k satisfy $H_k(\mathbf{x}) \leq 1$ and those belonging to a category other than class k, $H_k(\mathbf{x}) \geq -1$ [20]–[23].

IV. EXPERIMENTATION DESIGNS OF THE NON-INVERTING BUCK–BOOST DC–DC POWER CONVERTER SYSTEMS

In this section, we estimate the availability of the presented algorithms mentioned above to make dimensionality reduction and significant feature extraction in terms of incipient and serious faulty conditions subjected to different parameters of the capacitor. Intensive simulation and comparison studies for the non-inverting Buck–Boost DC–DC power converter systems are carried out under incipient fault and serious fault, respectively.

The two-dimensional (2-D) space visualisation results are shown in Figs. 2(a) and 2(b) (Scenario I), and Figs. 2(c) and 2(d) (Scenario II). In Figs. 2(a) and 2(b), the legends 'Fault 1', 'Fault 2', 'Fault 3', 'Fault 4', 'Fault 5', 'Fault
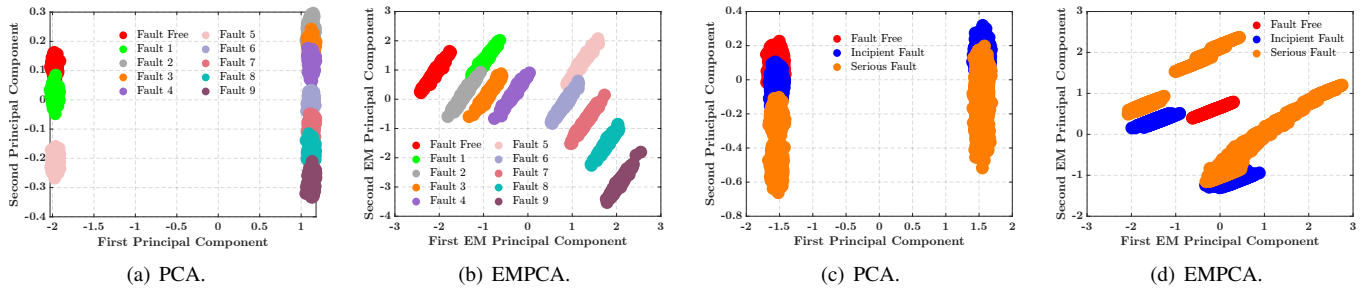
Fig. 2. 2-D space visualisation performances of fault classification for the non-inverting Buck–Boost DC–DC power converter systems under the projection onto Principal Component (PC) space in terms of data-driven and machine learning approaches. (a). Scenario I — PCA method; (b). Scenario I — EMPCA algorithm; (c). Scenario II — PCA method; (d). Scenario II — EMPCA algorithm.

TABLE I
CONFUSION MATRIX [20]–[23].

	Positive Predicted	Negative Predicted
Positive True	TP	FN
Negative True	FP	TN

6', 'Fault 7', 'Fault 8', and 'Fault 9' respectively represent the samples when the capacitor has effectiveness loss with 10.00%, 15.00%, 20.00%, 25.00%, 30.00%, 35.00%, 40.00%, 45.00%, and 50.00% respectively.

In Figs. 2(c) and 2(d), the legends 'Incipient Fault' and 'Serious Fault' respectively stand for the capacitor with the effectiveness losses varying from 80.00% to 90.00%, and from 50.00% to 79.00% with an interval of 1.00% , which means 80.00%, 81.00%, 82.00%, 83.00%, . . . , 89.00%, 90.00% represents the datasets of the 'Incipient Fault', and 50.00%, 51.00%, 52.00%, 53.00%, . . . , 78.00%, 79.00% stands for the datasets of the 'Serious Fault', respectively.

V. SIMULATION RESULTS

In this section, the performances of fault classification are presented using confusion matrices according to the projection onto *Principal Component* (PC) space. In diagnosis problems with negative (normal) and positive (abnormal) classes, data

samples for the negative class are easily obtained; nonetheless, those for the positive class are difficult to obtain. In such problems with imbalanced training data, misclassification of positive data into the negative category is fatal compared to misclassification of negative data into the positive class [20]–[23]. The confusion matrix for this problem has been shown in TABLE I, where *True Positive* (TP) is the number of correctly classified positive data, *False Negative* (FN) is the number of misclassified positive data, *False Positive* (FP) is the number of misclassified negative data, and *True Negative* (TN) is the number of correctly classified negative data [20]–[23].

Fig. 2 shows that the 2-D space visualisation performances of fault classification for the non-inverting Buck–Boost DC–DC power converter systems under the projection onto PC space. In order to validate the availability of the proposed algorithm, distinctive topologies of data-driven and machine learning-based fault classification approaches have been taken more into account.

The simulation results of Figs. 2(a) and 2(c) are based on data-driven and machine learning-based fault classification techniques using PCA, whereas the performances and characteristics illustrated in Figs. 2(b) and 2(d) aim to the proposed algorithm of EMPCA.

Fig. 3 (Scenario I) and Fig. 4 (Scenario II) demonstrate that the behaviours of fault classification based on the confusion

(a) Fault Classification using PCA + SVM.

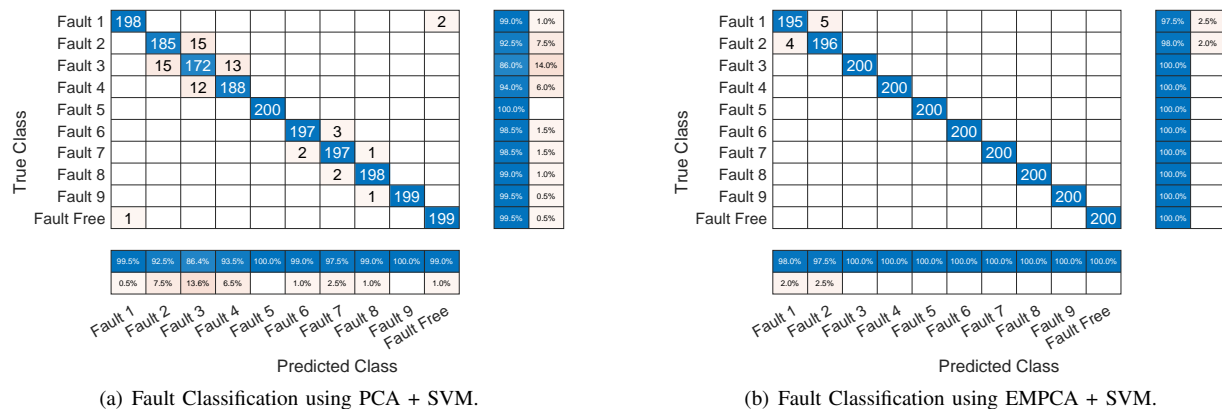(b) Fault Classification using EMPCA + SVM.

Fig. 3. Fault classification behaviours using confusion matrices for the non-inverting Buck–Boost DC–DC power converter systems depending on the projection onto PC space in terms of data-driven and supervised machine learning approaches — Scenario I. (a). PCA + SVM method; (b). EMPCA + SVM algorithm.
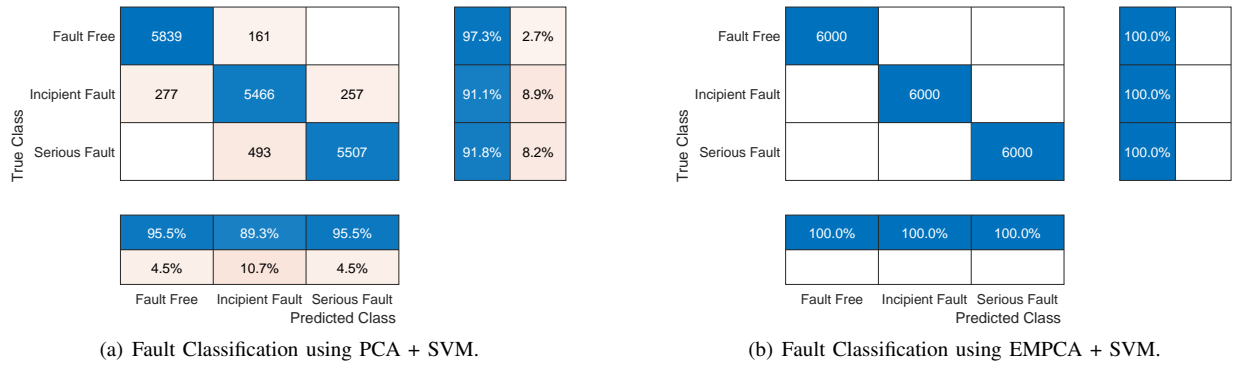
(a) Fault Classification using PCA + SVM.

(b) Fault Classification using EMPCA + SVM.

Fig. 4. Fault classification characteristics using confusion matrices for the non-inverting Bck–Boost DC–DC power converter systems relying on the projection onto PC space according to data-driven and supervised machine learning techniques — Scenario II. (a). PCA + SVM method; (b). EMPCA + SVM algorithm.

TABLE II
CONFUSION MATRICES PERFORMANCES DEPENDING ON THE PC SPACE PROJECTION FOR THE NON-INVERTING BUCK–BOOST
DC–DC POWER CONVERTER SYSTEMS USING PCA + SVM AND EMPCA + SVM TECHNIQUES — SCENARIO I.

| Healthy and FaultyModes | Confusion Matrices Performances of PC Space Projection Depending on Different Topologies of Data-Driven and Supervised Machine Learning Techniques for the Non-Inverting Buck–Boost DC–DC Power Converter Systems | | | | | | | |
| | PCA + SVM | | | | EMPCA + SVM | | | |
	TPR (%)	FPR (%)	PPV (Val. / No.)	FDR (%)	TPR (%)	FPR (%)	PPV (Val. / No.)	FDR (%)
Fault Free	99.0	1.0	199	0.5	**100.0**	—	**200.0**	—
Fault 1	**99.5**	**0.5**	**198**	**1.0**	98.0	2.0	195	2.5
Fault 2	92.5	7.5	185	7.5	**97.5**	**2.5**	**196**	**2.0**
Fault 3	86.4	13.6	172	14.0	**100.0**	—	**200**	—
Fault 4	93.5	6.5	188	6.0	**100.0**	—	**200**	—
Fault 5	100.0	—	200	—	100.0	—	200	—
Fault 6	99.0	1.0	197	1.5	**100.0**	—	**200**	—
Fault 7	97.5	2.5	197	1.5	**100.0**	—	**200**	—
Fault 8	99.0	1.0	198	1.0	**100.0**	—	**200**	—
Fault 9	100.0	—	199	0.5	100.0	—	**200**	—

matrices for the non-inverting Buck–Boost DC–DC power converter systems. In order to evaluate the feasibility of the proposed algorithm, distinctive topologies of data-driven and supervised machine learning-based fault classification methodologies have been taken more into considerations.

For one thing, the simulation results of Figs. 3(a) and 4(a) are based on data-driven and supervised machine learning-based fault classification techniques by combining and consolidating with PCA and SVM. For another thing, the performances shown in Figs. 3(b) and 4(b) concentrate on the proposed methodology of EMPCA + SVM.

Specifically, the functionality of the confusion matrices is to display the *True Positive Rates* (TPR) and *False Positive Rates* (FPR) in the row summary. Additionally, the *Positive Predictive Values* (PPV) and *False Discovery Rates* (FDR) will be shown in the column summary [20]–[23]. The fault

classification performances of the non-inverting Buck–Boost DC–DC power converter systems, which are based on intensive simulations and statistical criteria in confusion matrices, have been respectively demonstrated in TABLE II (Scenario I) and TABLE III (Scenario II), including TPR, FPR, PPV, and FDR with distinctive topologies of data-driven and supervised machine learning strategies of PCA + SVM and EMPCA + SVM.

VI. CONCLUSION

In this paper, the proposed algorithm of EMPCA Plus SVM has been adopted and applied to the non-inverting Buck–Boost DC–DC power converter systems for data-driven and supervised machine learning-based fault classification. The simulations have been carried out based on the incipient fault and serious fault, respectively. The comparison studies have been done, and the feasibility of the proposed methodology

TABLE III
CONFUSION MATRICES CHARACTERISTICS RELYING ON THE PC SPACE PROJECTION FOR THE NON-INVERTING BUCK–BOOST
DC–DC POWER CONVERTER SYSTEMS USING PCA + SVM AND EMPCA + SVM APPROACHES — SCENARIO II.

Healthy and Faulty Modes	Confusion Matrices Characteristics of PC Space Projection Relying on Contrasting Topologies of Data-Driven and Supervised Machine Learning Approaches for the Non-Inverting Buck–Boost DC–DC Power Converter Systems							
	PCA + SVM				EMPCA + SVM			
	TPR (%)	FPR (%)	PPV (Val./No.)	FDR (%)	TPR (%)	FPR (%)	PPV (Val./No.)	FDR (%)
Fault Free	95.5	4.5	5839	2.7	100.0	—	6000	—
Incipient Fault	89.3	10.7	5466	8.9	100.0	—	6000	—
Serious Fault	95.5	4.5	5507	8.2	100.0	—	6000	—

EMPCA + SVM has been well demonstrated. Additionally, EMPCA + SVM can not only distinguish the various classes of faulty conditions, but also identify the differences between the significant features within the same category. Specifically, it is worthy to point out, the proposed algorithm EMPCA + SVM outperforms the PCA + SVM for more sophisticated protocols. Furthermore, compared with PCA + SVM, the fault classification performances, illustrated in confusion matrices, have been obviously improved by using the EMPCA + SVM technique.

REFERENCES

[1] Z. Gao, C. Cecati, and S. X. Ding, "A survey of fault diagnosis and fault-tolerant techniques—part ii: Fault diagnosis with knowledge-based and hybrid/active approaches," *IEEE Transactions on Industrial Electronics*, vol. 62, no. 6, pp. 3768–3774, 2015.

[2] Z. Gao and X. Liu, "An overview on fault diagnosis, prognosis and resilient control for wind turbine systems," *Processes*, vol. 9, no. 2, 2021.

[3] R. Rahimilarki, Z. Gao, A. Zhang, and R. Binns, "Robust neural network fault estimation approach for nonlinear dynamic systems with applications to wind turbine systems," *IEEE Transactions on Industrial Informatics*, vol. 15, no. 12, pp. 6302–6312, 2019.

[4] E. Tian, D. Yue, and C. Peng, "Reliable control for networked control systems with probabilistic actuator fault and random delays," *Journal of the Franklin Institute*, vol. 347, no. 10, pp. 1907–1926, 2010.

[5] H. Wu, V. Pickert, X. Deng, D. Giaouris, W. Li, and X. He, "Polynomial curve slope compensation for peak-current-mode-controlled power converters," *IEEE Transactions on Industrial Electronics*, vol. 66, no. 1, pp. 470–481, 2019.

[6] H. Givi, E. Farjah, and T. Ghanbari, "Switch fault diagnosis and capacitor lifetime monitoring technique for dc–dc converters using a single sensor," *IET Science, Measurement & Technology*, vol. 10, pp. 513–527, 2016.

[7] Y.-K. Cho and K. C. Lee, "Noninverting buck–boost dc–dc converter using a duobinary-encoded single-bit delta-sigma modulator," *IEEE Transactions on Power Electronics*, vol. 35, no. 1, pp. 484–495, 2020.

[8] L. Jia, X. Sun, Z. Zheng, X. Ma, and L. Dai, "Multimode smooth switching strategy for eliminating the operational dead zone in noninverting buck–boost converter," *IEEE Transactions on Power Electronics*, vol. 35, no. 3, pp. 3106–3113, 2020.

[9] X. Weng, Z. Zhao, K. Chen, L. Yuan, and Y. Jiang, "A nonlinear control method for bumpless mode transition in noninverting buck–boost converter," *IEEE Transactions on Power Electronics*, vol. 36, no. 2, pp. 2166–2178, 2021.

[10] N. Rana and S. Banerjee, "Development of an improved input-parallel output-series buck-boost converter and its closed-loop control," *IEEE Transactions on Industrial Electronics*, vol. 67, no. 8, pp. 6428–6438, 2020.

[11] Y. Zhang, X.-F. Cheng, and C. Yin, "A soft-switching synchronous rectification noninverting buck–boost converter with a new auxiliary circuit," *IEEE Transactions on Industrial Electronics*, vol. 68, no. 9, pp. 7931–7937, 2021.

[12] A. Rodríguez-Lorente, A. Barrado, C. Calderón, A. Lázaro, and P. Zumel, "Magnetically coupled buck–boost bidirectional dc–dc converter," *IEEE Transactions on Industrial Electronics*, vol. 68, no. 10, pp. 9493–9504, 2021.

[13] G. Chen, Y. Liu, X. Qing, M. Ma, and Z. Lin, "Principle and topology derivation of single-inductor multi-input multi-output dc–dc converters," *IEEE Transactions on Industrial Electronics*, vol. 68, no. 1, pp. 25–36, 2021.

[14] Y. Fu, Z. Gao, and A. Zhang, "Data-driven parameter fault classification for a dc–dc buck converter," in *2021 6th International Symposium on Environment-Friendly Energies and Applications (EFEA)*, 2021, pp. 1–7.

[15] Y. Fu, Z. Gao, Y. Liu, A. Zhang, and X. Yin, "Actuator and sensor fault classification for wind turbine systems based on fast fourier transform and uncorrelated multi-linear principal component analysis techniques," *Processes*, vol. 8, no. 9, 2020.

[16] R. Vidal, Y. Ma, and S. Sastry, "Generalized principal component analysis (gpca)," *IEEE Transactions on Pattern Analysis and Machine Intelligence*, vol. 27, no. 12, pp. 1945–1959, 2005.

[17] S. Roweis, "Em algorithms for pca and spca," in *Proceedings of the 10th International Conference on Neural Information Processing Systems (NIPS)*. Cambridge, MA, USA: MIT Press, 1997, p. 626–632.

[18] M. Tipping and C. Bishop, "Mixtures of probabilistic principal component analyzers," *Neural Computation*, vol. 11, no. 2, p. 443–482, 1999.

[19] M. E. Tipping and C. M. Bishop, "Probabilistic principal component analysis," *Journal of the Royal Statistical Society: Series B (Statistical Methodology)*, vol. 61, no. 3, pp. 611–622, 1999.

[20] C. Cortes and V. Vapnik, "Support-vector networks," *Machine learning*, vol. 20, no. 3, pp. 273–297, 1995.

[21] A. Kumar, S. K. Singh, S. Saxena, A. K. Singh, S. Shrivastava, K. Lakshmanan, N. Kumar, and R. K. Singh, "Comhisp: A novel feature extractor for histopathological image classification based on fuzzy svm with within-class relative density," *IEEE Transactions on Fuzzy Systems*, vol. 29, no. 1, pp. 103–117, 2021.

[22] Q. Shi and H. Zhang, "Fault diagnosis of an autonomous vehicle with an improved svm algorithm subject to unbalanced datasets," *IEEE Transactions on Industrial Electronics*, vol. 68, no. 7, pp. 6248–6256, 2021.

[23] Y. Fu, Z. Gao, A. Zhang, and X. Liu, "Fault Classification for Wind Turbine Benchmark Model Based on Hilbert–Huang Transformation and Support Vector Machine Strategies," in *2021 IEEE 19th International Conference on Industrial Informatics (INDIN)*, 2021.